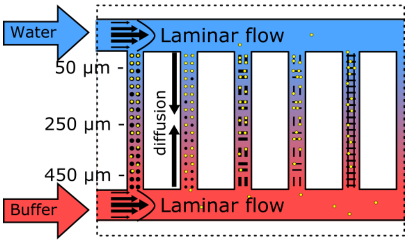

SLS Symposium on

Micro and nano-structures

Tuesday, October 11, 2016

10:00 to 11:45, WBGB/019

10:00 Enabling next generation lithography at the XIL beamline: from single-digit resolution to materials characterization.
Roberto Fallica, E. Buitrago, Y. Ekinci

10:30 Nanofluidic trapping devices for detecting critical reaction concentrations
Michael A. Gerspach, D. Sharma, N. Mojarad, T. Pfohl, Y. Ekinci

11:00 Coffee

11:15 The 25 µm pitch MOENCH detector for low energies and high resolution
Marco Ramilli, A. Bergamaschi, M. Brückner, S. Cartier, R. Dinapoli, E. Fröjdh, D. Greiffenberg, C. Lopez, D. Mezza, A. Mozzanica, S. Redford, M. Ruat, C. Rüder, B. Schmitt, X. Shi, G. Tinti, D. Thattil, J. Zhang

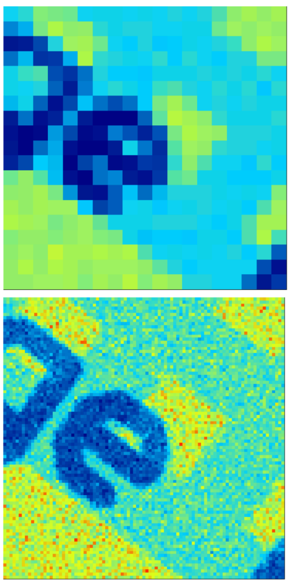

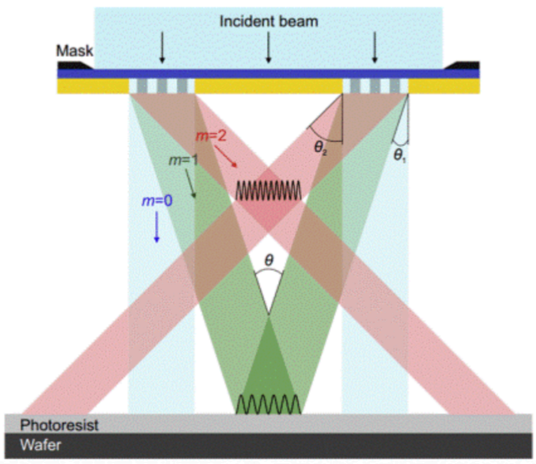

Enabling next generation lithography at the XIL beamline: from single-digit resolution to materials characterization.

Roberto Fallica, Elisabeth Buitrago, Yasin Ekinci
Paul Scherrer Institut, 5232 Villigen PSI, Switzerland

Next generation lithography for the mass production of integrated circuits will be based on extreme ultraviolet (EUV) light at 13.5 nm, which is a significant improvement over the current technology based on deep ultraviolet light at 193 nm. EUV lithography will enable higher resolution, simplification of process and lower cost-per-wafer in comparison to the latter. However, the transition to EUV demands both the design of novel photosensitive materials and a solid understanding of the physicochemical processes occurring in this regime.

At the XIL beamline of the SLS we test the patterning performance of photoresists by use of the EUV interference lithography tool which is capable of unparalleled single-digit resolution patterning[1,2]. The schematic principle of operation is shown in the Figure (top); scanning electron images of high resolution patterns are also shown (at bottom). The XIL is being extensively used for pre-screening of novel photoresists under development in academia and industry. As a result, we had the opportunity to test a wide range of materials: from the chemically amplified resists with polymer backbone, to the photocondensed tin-based metal oxides, to carbon-based molecular compounds. In this overview, the advantage and disadvantage of each approach and the various applications will be presented. I will also present and discuss the challenges in terms of lithographic sensitivity, sidewall roughness and resolution needed to meet the target specification required by adoption at the 7 nm technological node. Besides its industrial importance, the study of photoresists opens new possibilities in patterning schemes and insight for research centers as well. In the last part of my talk, I will present a methodology to measure the absorption coefficient at EUV of photoresists and to extract the reaction rate and kinetics during exposure by *in situ* transmission measurement.

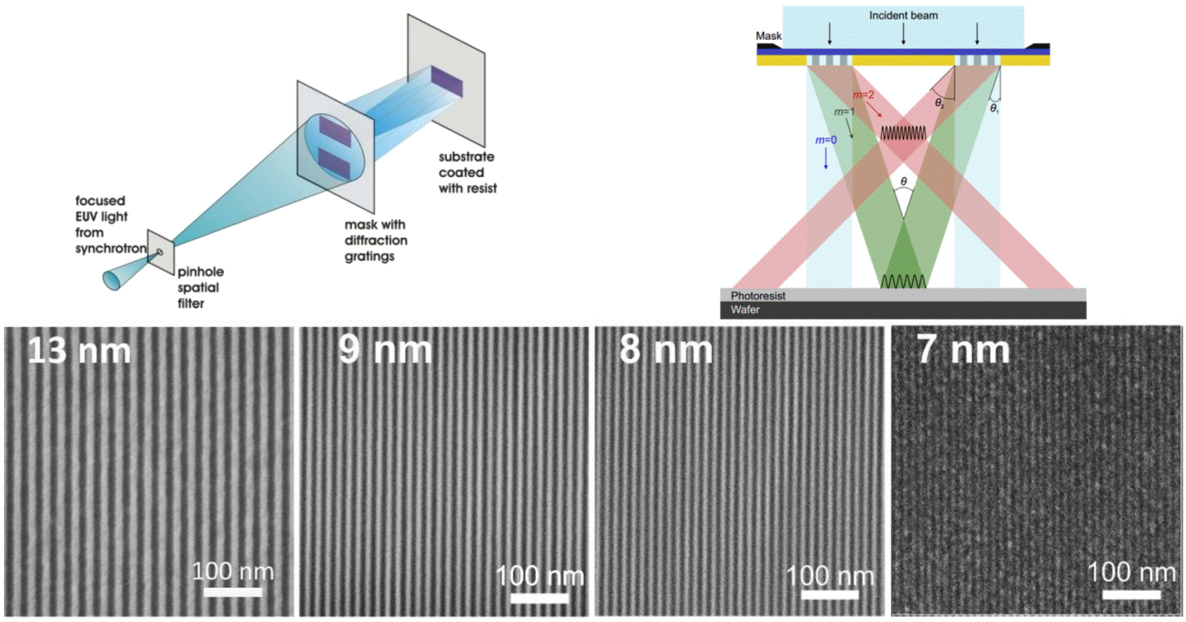

References

[1] N. Mojarad, J. Gobrecht, and Y. Ekinci, Microelectronic Engineering 143, 55 (2015).
[2] D. Fan and Y. Ekinci, Journal of Micro/Nanolithography, MEMS and MOEMS 15(3), 033505 (2016).

Nanofluidic trapping devices for detecting critical reaction concentrations

Michael A. Gerspach [a,b,c], Deepika Sharma [a,b], Nassir Mojarad [b,d], Thomas Pfohl [a,c], Yasin Ekinci [a,b]

[a] Swiss Nanoscience Institute, Basel, 4056, Switzerland
[b] Paul Scherrer Institute, Villigen, 5323, Switzerland
[c] Department of Chemistry, University of Basel, Basel, 4056, Switzerland
[d] ETH Zürich, Nanotechnology group, Säumerstrasse 4, 8803 Rüschlikon, Switzerland

The ultimate limit to analytical sensitivity at the nanoscale is the reliable detection and trapping of single nano-objects, which provide information on local dynamics and reactions. Extensive developments in active trapping methods such as optical and magnetic tweezers have been successfully demonstrated stable confining of single objects. However, they often need demanding setups and externally applied forces to create a trap defining field gradient. An alternative method of passively trapping and detecting objects smaller than 100 nm is geometry induced electrostatic (GIE) trapping [1, 2].

In GIE trapping, single negative charged nano-objects are trapped by electrostatic repulsion from negatively charged walls in nano-channels (figure 1). By altering the surface topology of the nano-channels, local energy potential wells can be created. If a particle then falls into such a potential well, it is reliably trapped from milliseconds to several minutes depending on the trap stiffness. The trap stiffness can be controlled by modifying the trap dimensions, nano-channel height, the charge density of the object and the device surface, and by changing ionic strength of the buffer solution. [1, 2]. Current GIE trapping devices for higher signal-to-noise detection are fabricated from glass substrates using state-of-the-art top-down nano-fabrication.

Integrating GIE trapping into microfluidic systems provides many advantages, including very small sample and reagent quantities, precise control of reactant concentrations as well as short analysis time. Furthermore, using a straightforward microfluidic design, a precise controlled steady state concentration gradient, e.g. of reactants or salt, can be formed over the area where the nano-objects are trapped as shown in figure 1 and 2. The gradient in the trapping region (nano-channels) is created by flowing two different solutions through the upper and lower supporting micro-channels, respectively. Since the two supporting channels are only connected through the nano-channels, a steady state gradient is formed in the GIE trapping area by diffusion.

The stiffness of the traps is reduced by increasing the salt concentration in the buffer solution due to the screening of the surface charges by free counter ions. For demonstration, a salt gradient from 0.05 mM to 1.0 mM NaCl was formed in the nano-channels and the trap stiffness along one nano-channel were measured using 60 nm gold nanoparticles. The trapped gold particles were recorded at different positions in the nano-channel (figure 2). From lateral probability distributions of the particles confined in the traps, the radial stiffness can be calculated as shown in figure 3. As the salt concentration along the nano-channel is increased, the stiffness of the traps is reduced from 0.08 pN/nm at 0.15 mM ionic strength to 0.006 pN/nm at 0.91 mM.

GIE trapping devices integrated into a gradient forming microfluidic system enable simple and high throughput trapping of nano-objects for studying their behavior and determine critical reaction concentrations of reactants on single trapped nano-objects. Furthermore, buffer solutions can be easily exchanged during the experiment by flushing through the supporting micro-channel, simplifying our further studies and opens the possibility for surface functionalization to increase the trap stiffness or reverse the charge for trapping positively charges nano-objects.

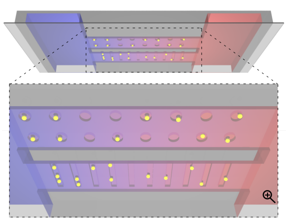

Figure 1. Schematic of nano-objects trapped along a steady linear reactant gradient by combining GIE trapping devices with a microfluidic design.

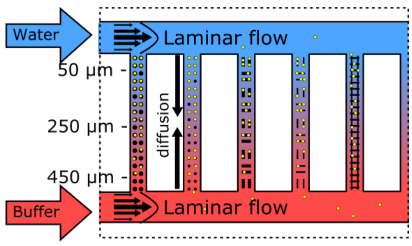

Figure 2. A steady state gradient in the trapping region is formed by simple diffusion of the salt ions from the two buffer solutions flowing through the supporting channels. Thus the analysis of single nano-objects at different concentrations is achieved within a single device.

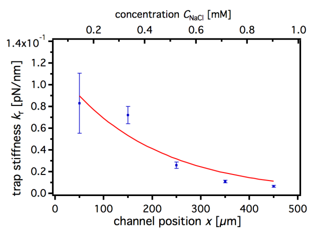

Figure 3. Trap stiffness of 60 nm gold particles recorded at different positions in the nano-channel. The higher the ionic strength of the solution, the less strong the particles are confined in the traps.

References

[1] M. Krishnan, N. Mojarad, P. Kukura and V. Sandoghdar, Geometry-induced electrostatic trapping of nanometric objects in a fluid, Nature 457 (2010), 692-695

[2] M. Gerspach, N. Mojarad, T. Pfohl and Y. Ekinci, Glass-based geometry-induced electrostatic trapping devices for improved scattering contrast imaging of nano-objects, Microelectronic Engineering 145, 43-48 (2015)

The 25 μm pitch MÖNCH detector for low energies and high resolution

M.Ramilli, A.Bergamaschi, M.Brückner, S.Cartier, R.Dinapoli, E.Fröjdh, D.Greiffenberg, C. Lopez, D.Mezza, A.Mozzanica, S. Redford, M. Ruat, C. Rüder, B.Schmitt, X.Shi, G.Tinti, D. Thattil, J. Zhang

SLS Detector Group, Paul Scherrer Institut, 5232 Villigen PSI, Switzerland

MÖNCH is a research project which aims to push the development of hybrid pixel detectors to its limits in terms of photon flux, position resolution, energy information and low energy detection. It features a charge integrating pixel architecture, compressed in a 25 μm pixel pitch. Its finer granularity grants higher intrinsic spatial resolution and its lower pixel capacitance allows for higher readout rates and low noise levels. However, the small pixel pitch implies an increased difficulty in bump bonding and an almost constant charge sharing between neighboring pixels, which in case of MÖNCH happens in $\sim$90% of the cases [1]. In the last two years the prototypes 02 and 03 have been systematically characterized.

The bump bonding is performed in-house and latest encouraging result give a yield better than 99.95%. The pixel charge sharing has been exploited to reconstruct the photon interaction point via a two-dimensional interpolation algorithm, based on a generalization of the η distribution used for strip detectors. As a result, when used in single-photon regime, MÖNCH can achieve a position resolution of the order of 1 μm [2]. This high resolution has been used in several proof-of-principle experiments with grating interferometry without the use of an analyzer grating.

Noise characterization of MÖNCH prototype provided fairly low values, reaching the $\sim$38 ENC [2] for the high gain setting, therefore setting a lower bound for the detector sensitivity in energy at energies below the 1 keV level and making it an interesting candidate for soft X-ray detection. A first test of its energy reconstruction and imaging capabilities have been conducted in the energy range between 1.75 keV and 3.5 keV at the PHOENIX beam line, and results will be presented.

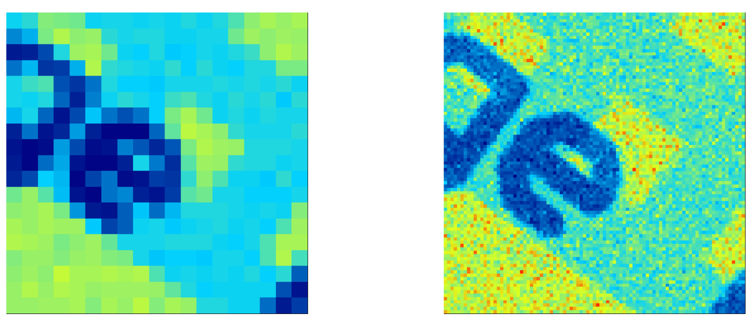

Figure 1: Examples of MÖNCH position resolution. Left: absorption image of an HDI, in photon counts per pixel. Right: same image, after position interpolation, with 1 μm bins.

References

[1] S. Cartier et al., JINST10 C03022 (2015).

[2] S. Cartier et al., JINST9 C05027 (2014).